https://dx.doi.org/10.21577/0103-5053.20230064

J. Braz. Chem. Soc., Vol. 34, No. 10, 1509-1519, 2023

Article

Preparation of Composite Films of Sodium Alginate-Based Extracted from Seaweeds *Macrocystis pyrifera* and *Lessonia trabeculata* Loaded with Aminoethoxyvinylglycine

Nelson Adrián Villacrés,[a] *Eder T. G. Cavalheiro,*[b] *Carla C. Schmitt,*[b] *Tiago Venâncio,*[c] *Hugo A. Alarcón*[a] *and Ana C. Valderrama*[*,a]

[a]*Faculty of Sciences, National University of Engineering, 15333 Rimac-Lima, Peru*

[b]*Instituto de Química de São Carlos, Universidade de São Paulo, 13566-590 São Carlos-SP, Brazil*

[c]*Laboratório de Ressonância Magnética Nuclear, Departamento de Química, Universidade Federal de São Carlos, 13565-905 São Carlos-SP, Brazil*

Composite films are an alternative in the replacement of synthetic polymers. These films can be prepared from polysaccharides and used to store various drugs to be applied in different areas. In addition, aminoethoxyvinylglycine (AVG) is an ethylene inhibitor that prolongs shelf life of food. For this reason, this research aimed to take advantage of the brown algae *Macrocystis pyrifera* and *Lessonia trabeculata* to extract sodium alginate and produce films composed of sodium alginate/kappa-carrageenan/iota-carrageenan, which were plasticized with glycerol and polyethylene glycol 400 and loaded with aminoethoxyvinylglycine. The extracted sodium alginate was characterized by ^{1}H and ^{13}C nuclear magnetic resonance (NMR), size exclusion chromatography coupled with multi-angle light scattering (SEC-MALS), thermogravimetry (TG/DTG), Fourier transform infrared (FTIR), and X-ray diffraction (XRD); and the composite films were characterized by FTIR, XRD, TG/DTG, and scanning electron microscopy (SEM). Then, the drug release kinetics were investigated using Higuchi and Korsmeyer-Peppas kinetic models. The extracted alginates obtained were of low molecular weight, and the films showed desirable properties for AVG release. Furthermore, drug release profiles revealed that AVG release is governed by Fick's Law, and this is favored at low temperatures. In summary, sodium alginate allows the preparation of composite films, which can replace synthetic polymers to be used in the loading and releasing of drugs.

Keywords: *Macrocystis pyrifera*, *Lessonia trabeculata*, sodium alginate, film, aminoethoxyvinylglycine

Introduction

Polymeric materials are massively used for almost one hundred years. However, around 99% of the raw materials used in the production of plastics come from non-renewable resources. For this reason, concern has arisen about the sustainability of these materials due to their low degradability and accumulation in the environment.[1] Due to their renewability and sustainability, several research has focused on the use of seaweed polysaccharides for film development. Among the polysaccharides used, alginate, carrageenan, and agar stand out.[2]

Alginate is a rigid, edible, and renewable polysaccharide used to encapsulate bioactive molecules[3] and in the production of films. It is extracted from brown algae[4] and represents 40% of the total dry weight of algae.[5] At the molecular level (Figure 1a), alginate is a linear polymer formed by monomers of β-D-mannuronic acid (M) and α-L-guluronic acid (G) linked by a (1-4) bond, which form M-, G-, and MG-sequential blocks. The sequence of monomers (M and G) differs between species of algae and within tissues of the same species. Furthermore, the M/G ratio and the composition and alternation in the M-G blocks determine the physicochemical properties of alginates.[6] For example, a high proportion of GG blocks results in harder and more brittle alginate films, while a high content of MG blocks forms softer gels and more elastic films.[7]

Carrageenan is an anionic linear polysaccharide (contains 15-40% sulfate ester groups). It is made up of

*e-mail: ana.valderrama.n@uni.edu.pe
Editor handled this article: Fernando C. Giacomelli (Associate)

D-galactose and 3,6-anhydro-galactose (3,6-AG) units linked by alternating α-1,3 and β-1,4 glycosidic bonds; and represents between 30 and 75% of the dry weight of red algae. It is classified into six basic forms according to its sulfate content, extraction source, and solubility; the most important being kappa-carrageenan (Figure 1b), iota-carrageenan (Figure 1c), and lambda-carrageenan.[8] Kappa-carrageenan (κ-carrageenan) presents ca. 25-30% sulfate content, and iota-carrageenan (ι-carrageenan) presents around 28-30%.[9]

Many studies[10] have been reported on the combination of two or more polysaccharides to improve the physical and mechanical properties of films. The compatibility in the mixture of different polysaccharides results in a compact and stable network which influences the properties of the film.[11] These composite films can be used as carriers for antioxidants, antimicrobial agents, flavors, colorants,[12] and ethylene retarders to control postharvest losses and food quality deterioration.[13]

Ethylene plays an important role in the ripening of fruits. Their synthetic pathway is controlled by the enzymes 1-aminocyclopropane-1-carboxylic acid (ACC) synthase and ACC oxidase, for this reason, they are targets for chemical inhibitors.[14] Therefore, aminoethoxyvinylglycine (AVG) and aminoisobutyric acid (AIB) are used to inhibit ACC synthase and ACC oxidase activity, respectively.[15]

Considering the need for and importance of developing films made from natural resources, this research focused on the extraction of sodium alginate from the brown algae species *Macrocystis pyrifera* and *Lessonia trabeculata* to make composite films loaded with an ethylene inhibitor and to study its release kinetics.

Experimental

Materials

The raw materials used in the extraction and preparation of the composite films were brown algae *Macrocystis pyrifera* and *Lessonia trabeculata* collected 3 km west of the San Juan de Marcona pier, Ica-Peru. Glycerol, average weight poly(ethylene glycol) Mn 400 (PEG 400), κ-carrageenan, ι-carrageenan and aminoethoxyvinylglycine hydrochloride were purchased from Sigma-Aldrich (St. Louis, USA). Ethanol, *n*-hexane, formaldehyde, sodium carbonate, calcium chloride, hydrochloric acid and sodium hydroxide were from Merck (Darmstadt, Germany). Commercial chemicals were of analytical grade and no further purification was employed.

Sodium alginate extraction

Sodium alginate (NaAlg) extraction was performed according to Gómez *et al.*[16] and Fertah *et al.*[6] with some modifications. In an amber bottle, 50 g ground-dried seaweed blades were mixed with 600 mL of *n*-hexane and allowed to macerate for 24 h to degrease the sample; then, the solid was filtered and soaked for 24 h at room temperature with 600 mL of 0.1% formaldehyde (v v^{-1}) to remove pigments. After that, the degreased and depigmented solid was mixed with a 3% Na_2CO_3 solution (m v^{-1}) at 80 °C for 2 h until reaching a pH value of 10. The liquid phase was separated by centrifugation and added slowly in 96° ethanol, forming a precipitate that was filtered and dried in an oven at 45 °C. The precipitate was mixed with 200 mL of 0.05 M $CaCl_2$ solution under constant stirring for 24 h at room temperature; then centrifuged and acidified with a 0.1 M HCl solution

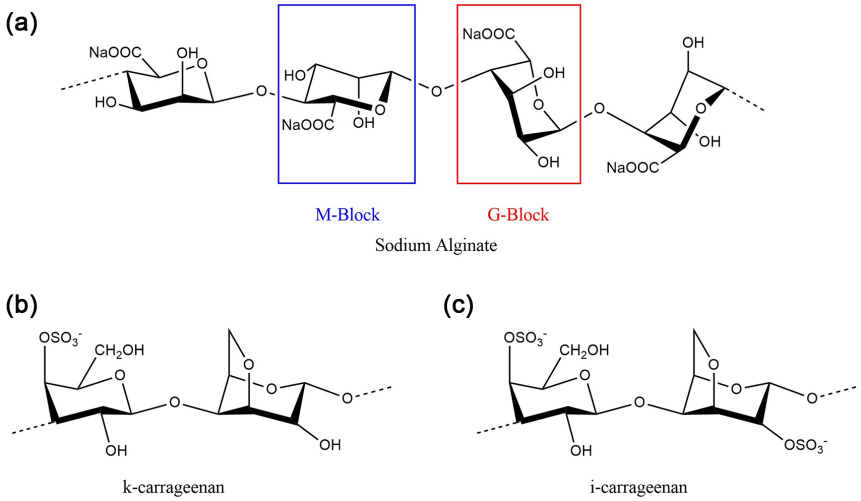

Figure 1. (a) Representation of alginate chemical structure and block distribution, (b) kappa-carrageenan chemical structure, and (c) iota-carrageenan chemical structure.

(pH ca. 2) to obtain alginic acid, which by basic treatment with a 0.1 M NaOH solution (pH ca. 8) was converted into sodium alginate (NaAlg). NaAlg was precipitated with 96° ethanol, filtered, and lyophilized. The sodium alginate yield was calculated as follows:

$$\text{Yield of sodium alginate (\%)} = \frac{\text{weight of alginate}}{\text{weight of brown algae dried biomass}} \times 100 \quad (1)$$

Preparation of film-forming solution and films loaded

The preparation of sodium alginate/κ-carrageenan/ι-carrageenan composite films loaded with AVG was carried out using the methodologies developed by Cha *et al.*[17] and Paula *et al.*[18] Thus, 30 mL of sodium alginate at 1.5% m v^{-1} were mixed with 5 mL of κ-carrageenan (1.0% m v^{-1}) and 5 mL of ι-carrageenan (1.0% m v^{-1}) for 60 min at 70 °C. Then, 1 g of the mixture of glycerol and PEG 400 in 9:1 ratio m/m was added and stirred for 30 min at 50 °C. Subsequently, 10 mL of AVG in ethanol (20 mg L^{-1}) was added and stirred for 30 min at 50 °C. Finally, the solution was poured into a Petri dish and dried at 50 °C for 24 h. This procedure was performed for each sample of sodium alginate extracted, obtaining two composite films.

AVG release

The study of the release kinetics of the ethylene inhibitor (aminoethoxyvinylglycine-AVG) was carried out at 10 and 25 °C in an ethanol 70° release medium to evaluate the thermosensitivity of the films. A DaiHan MaXircu™ CR-8 Refrigerating/Heating Bath Circulator was used to control the release temperature, coupled to a digital orbital shaker, WiseShake® SHO-2D, containing 50 mL borosilicate glass double layer jacketed Beakers. For measurement purposes, a 2 mL aliquot of the release medium was removed to determine its absorbance at 197.5 nm in a quartz cuvette with 1.0 cm optical pass on a UV-1800 UV-Vis spectrophotometer (Shimadzu, Japan). After, the aliquot was returned to the release medium and the release system was kept stirring. This process was repeated at each predetermined times. The Higuchi (equation 2) and Korsmeyer-Peppas (equation 3) equations were used to assess whether Fick's law governs diffusion processes.

The Higuchi model describes the diffusion of the drug on only one side of the film, where the swelling and dissolution processes are negligible. Furthermore, this model considers a constant diffusivity of the drug with ideal sink conditions in the release environment.[19] The Higuchi release equation is given by:

$$\frac{M_t}{M_\infty} = K_H \times t^{0.5} \quad (2)$$

where M_t/M_∞ is the fraction of solute released at time t and K_H is the Higuchi diffusion constant.

The Korsmeyer-Peppas model is used to determine the value of the release exponent "n". When this value is 0.5, it indicates that the release is carried out by drug diffusion. Likewise, when the value of n is less than 0.5, it indicates that the diffusion process is controlled by Fick's law; and above 0.5 that the diffusion does not obey this law and is caused by polymer erosion.[20] The Korsmeyer-Peppas equation is given by:

$$\frac{M_t}{M_\infty} = K \times t^n \quad (3)$$

where K is the system constant and n is the diffusion exponent.

Characterization

^{1}H nuclear magnetic resonance spectroscopy (^{1}H NMR)

^{1}H NMR spectra were obtained using 12 mg of sample dissolved in 1.2 mL of a solution of D_2O and 3 mM trimethylsilylpropanoic acid (TSP) at 70 °C. A Avance III HD 500 MHz (Bruker, Germany) coupled with an Ascend 11.75 T superconducting magnet (500 MHz) was used. The signal (δ) referring to the TSP internal reference standard is at 0.00 ppm, and the residual signal from the D_2O solvent is at 4.32 ppm.

The M/G ratio and the values of the molar fractions F_G, F_M, F_{GG}, F_{MM}, F_{MG}, and F_{GM} were calculated from the area of ^{1}H NMR signals, employing the formulas given by Rashedy *et al.*[21]

$$F_G = \frac{A_I}{A_{II} + A_{III}} \quad (4)$$

$$F_M = 1 - F_G \quad (5)$$

$$F_{GG} = \frac{A_{III}}{A_{II} + A_{III}} \quad (6)$$

$$F_{GM} = F_{MG} = F_G - F_{GG} \quad (7)$$

$$F_{MM} = F_M - F_{MG} \quad (8)$$

$$M/G = \frac{(1 - F_G)}{F_G} \quad (9)$$

$$\eta = \frac{F_{MG}}{F_M \times F_G} \quad (10)$$

A_I corresponds to the anomeric hydrogen of guluronic acid (5.0-5.2 ppm), A_{II} to the anomeric hydrogens of mannuronic acid (4.6-4.8 ppm), and A_{III} to the guluronic acid residues in the homopolymeric G blocks (4.4-4.5 ppm).

The parameter η evaluates and reveals the sequence distribution of the M and G blocks. Indeed, the values of $\eta < 1$ correspond to the abundance of homopolymeric MM and GG blocks, $\eta = 1$ for completely random cases and $1 < \eta < 2$ for alternate-like cases MG and GM.[22]

^{13}C nuclear magnetic resonance spectroscopy

^{13}C NMR spectra were obtained using 60 mg of sample in powder form packed in zirconia rotors with an external diameter of 4 mm. A Avance III-400 NMR spectrometer (Bruker, Germany) was used, operating at a 9.4 T magnetic field. The resonance frequency was 100.56 MHz with a sequence of CPTOSS pulses (cross polarization with total sideband suppression) and MAS-BB-4 mm probe. The signal (δ) corresponding to the chemical shift calibration standard (adamantane) is observed at 38.5 ppm.

Average mol mass

The molecular weight was evaluated by size exclusion chromatography coupled with multi-angle light scattering (SEC-MALS) using a e2695 chromatograph (Waters, Massachusetts, USA) with Wyatt miniDawn and Optilab model detectors, Shodex brand LB-803 and LB-806 columns and at a temperature of 35 °C.

The SEC-MALS analysis was performed according to the ASTM F2605-16 standard.[23] The mobile phase of Na_2SO_4 (0.05 M)/ethylenediaminetetraacetic acid (EDTA) (0.01 M) at pH 6.0, pullulan standard solutions, and 200 µL of the sample at a concentration of 5 mg mL^{-1} were used. The processed data were with Astra v. 7.3.0.15 using the value of the increase in the specific refractive index of the solution (dn/dc) of 0.150 mL g^{-1}.

Thermogravimetry (TG/DTG)

The thermogravimetric curves were obtained in a SDT Q600 (TA Instruments, Delaware, USA) equipment managed by the Thermal Advantage for Q Series software (v. 5.5.24). Measurements were performed using an inert atmosphere (N_2) at a flow rate of 50 mL min^{-1} using 5.0 ± 0.2 mg of sample. The temperature range was from 25 to 1000 °C with a heating rate of 10 °C min^{-1} and in open α-alumina sample supports.

Fourier-transform infrared spectroscopy (FTIR)

The FTIR spectra were obtained by attenuated total reflectance (ATR) using an IRPrestige 21 spectrophotometer (Shimadzu, Kyoto, Japan), from 600 to 4000 cm^{-1}, after the acquisition of 20 scans at a resolution of 4 cm^{-1} for each spectrum.

X-ray diffraction (XRD)

The XRD diffractograms have obtained in a range from 5 to 100° in a D8 Advance (Bruker, Germany) equipment equipped with a Cu source (Kα = 1.5418 Å) operating at a voltage of 40 kV and 40 mA (1600 W) and a LynxEye model PSD type detector. Measurements were performed in coupled Theta/2Theta mode with continuous sweep and 0.02° increment and 0.5 s accumulation time *per* step. A Ni filter has been used to remove the signal associated with Kβ radiation. The crystallinity index was determined using the ratio of the crystalline area and the total area (equation 11).

$$\text{Crystallinity}\ (\%) = \frac{\text{crystalline area}}{\text{total area}} \times 100 \qquad (11)$$

Surface morphology

The surface of the films was observed by scanning electronic microscopy using an S-440 microscope (LEO, Cambridge, England) equipped with a 7060 detector (Oxford Instruments, England) and at resolutions of 10 and 1 µm at 1000× and 5000× magnification, respectively. Before visualization, the samples were gold-plated in a MED 020 high vacuum metallizer (Bal-Tec, Liechtenstein).

Results and Discussion

Sodium alginate extracted

Alginate extracted from *Macrocystis pyrifera* was named NaAlgM, and from *Lessonia trabeculata* was named NaAlgL, respectively.

Sodium alginate yield

The sodium alginate yield for the brown seaweed blades was determined. The highest alginate content (22.24% dry weight (dw)) was obtained of *L. trabeculata*, and the lower alginate content was recorded on *M. pyrifera* (15.28% dw). Kaidi *et al.*[24] report a sodium alginate extraction yield from *L. trabeculata* between 13-29% dw and from *M. pyrifera* between 18-45% dw. However, according to Rioux *et al.*,[25] the sodium alginate extraction yield in *M. pyrifera* is 1-21% dw. Dobrinčićet *et al.*[26] report that this difference in extraction yield percentage varies with algae age, environmental growth conditions (e.g., light, temperature, and nutrients), and extraction techniques.

NMR spectroscopy analysis

Analysis of the ^{1}H NMR spectra (Figure 2) allowed the determination of the mannuronate/guluronate (M/G) ratio of the sodium alginate samples. Quantitatively, this was done by associating the area of the respective peaks with the F_M and F_G molar fractions. Table 1 shows that NaAlgM has an M/G ratio of 1.00 and NaAlgL of 0.86. However, the M/G ratio of NaAlgM is lower than that reported by Murillo and Hernández,[27] who obtained a value of 1.63; in addition, the M/G ratio of NaAlgL is higher than that reported by Venegas *et al.*,[28] which obtained a value of 0.61. McKee *et al.*[29] mention that the M/G ratio differs significantly according to the age of the leaves and the environmental conditions the algae inhabit.

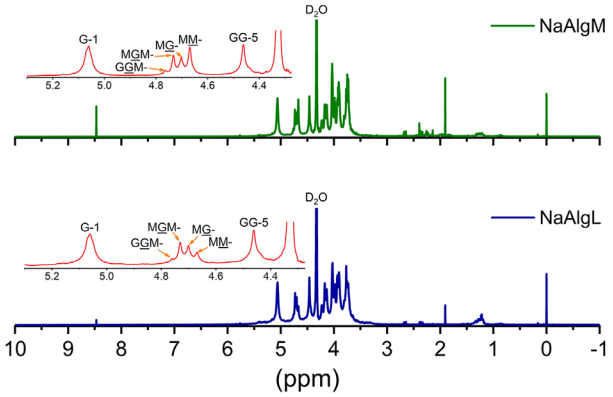

Figure 2. ^{1}H NMR spectra (500 MHz, D_2O) of sodium alginate samples extracted from *M. pyrifera* (NaAlgM, green line) and *L. trabeculata* (NaAlgL, blue line).

The gelling properties of the alginate depend on the M/G ratio and the molar frequency of the blocks F_{MM}, F_{GG}, F_{MG}, and F_{GM}. These parameters influence the chemical and physical properties of the alginate, making the stiffness proportional to the content and length of the G blocks (F_G) and increase in the following order: MM block < MG block < GG block,[24] showing that NaAlgL is more rigid than NaAlgM, as shown in Table 1. Furthermore, the sequence distribution was described by η value. In Table 1, the values slightly exceeded one in the extracted alginates reflecting a probably random composition of the MG/GM heteropolymeric fractions in the structure and composition of their polymeric matrices.

In the ^{13}C NMR spectra (Figure 3) the peak between 170 and 180 ppm corresponds to the carboxyl carbon atom (C_6), and the signal of the C_1 anomeric carbon is located between 90 and 110 ppm. On the other hand, the signals of the ring carbons of pyranose (C_2, C_3, C_4, and C_5) are 60 to 90 ppm.[30] These peaks are labeled A-G, and each carbon assignment is shown in Table 2. In addition, the region between 160 to 170 ppm shows some peaks which coincide with the protonated carboxyl groups, which reflects the conversion of $COO^{-}\cdots X^{n+}$ groups to protonated COOH units.[31] Peak assignments for ^{13}C NMR spectra signals are presented in Table 2.

Average mol mass

Average mol mass and polydispersity index were obtained by SEC-MALS (Figure 4). The average mol mass (M_w) of the NaAlgM and NaAlgL samples was 6.519×10^4 and 6.791×10^4 g mol^{-1}, respectively. Deng *et al.*[32] report that the average mol mass of alginate is in the range of $3.2\text{-}40 \times 10^4$ g mol^{-1}, which shows that the extracted sodium alginate samples are of low molecular weight. The polydispersity index was found to be 1.418 for NaAlgM and 1.528 for NaAlgL. The ratio between the weight-average mol

Table 1. Composition data of sodium alginate samples extracted from *M. pyrifera* (NaAlgM) and *L. trabeculata* (NaAlgL)

Sample	Composition		Ratio M/G	Sequence			η
	F_M	F_G		F_{MM}	F_{GG}	$F_{MG,\ GM}$	
NaAlgM	0.50	0.50	1.00	0.24	0.24	0.26	1.05
NaAlgL	0.46	0.54	0.86	0.21	0.28	0.25	1.02

M: β-D-mannuronic acid; G: α-L-guluronic acid; F_G, F_M, F_{GG}, F_{MM}, F_{MG}, and F_{GM}: molar fractions; η: parameter to evaluate the sequence distribution of the M and G blocks.

Table 2. Peak assignments of the ^{13}C resonances designated A-G in Figure 3

	Peak designation						
	A	B	C	D	E	F	G
Chemical shift / ppm	176.2	102.4	82.8	76.3	71.6	68.1	65.1
Residue assignment	G, M	G, M	G	M	M	G	G
Carbon atom	6	1	4	4,5	2,3	3,5	2

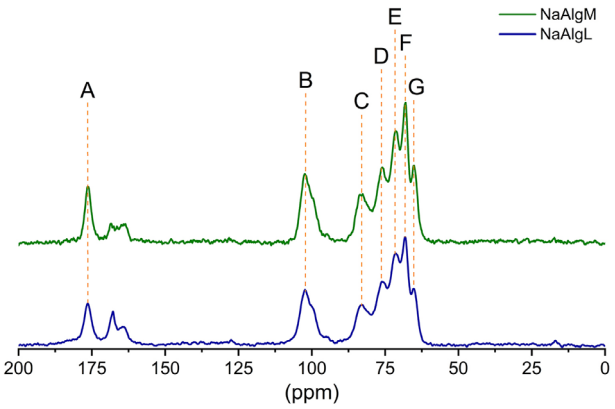

Figure 3. ^{13}C NMR spectra (400 MHz) of sodium alginate samples extracted from *M. pyrifera* (NaAlgM, green line) and *L. trabeculata* (NaAlgL, blue line).

mass (M_w) and the number-average mol mass (M_n) defines the polydispersity index (PDI or Đ). When PDI is equal to 1, the samples are monodisperse, and when the value is greater than unity, the samples are polydisperse.[33] This shows that the samples of sodium alginate extracted from brown algae are polydisperse. These results are supported by Boucelkha *et al.*,[34] who reported that the PDI values of the extracted alginate samples vary between 1.4 and 6.0 due to the extraction and purification processes. Table 3 shows the values of molar mass and polydispersity index.

Table 3. Average mol mass (M_n and M_w) and polydispersity index (PDI) of sodium alginate samples extracted from *M. pyrifera* (NaAlgM) and *L. trabeculata* (NaAlgL)

Sample	$M_w \times 10^4$ / (g mol^{-1})	$M_n \times 10^4$ / (g mol^{-1})	PDI
NaAlgM	6.519 (± 2%)	4.597 (± 4%)	1.418 (± 5%)
NaAlgL	6.791 (± 2%)	4.444 (± 2%)	1.528 (± 3%)

Thermogravimetry

Figure 5 shows the TG/DTG curves of the samples NaAlgM (Figure 5a) and NaAlgL (Figure 5b) in which the four thermal events occur during the thermogravimetric test of the sodium alginate samples. In these events, the processes of dehydration, fragmentation of the alginate into monomeric units, decomposition of monomeric units into carbonate, and carbonization are carried out.[35] The results obtained from the TG/DTG thermograms of the alginate samples are shown in Table 4.

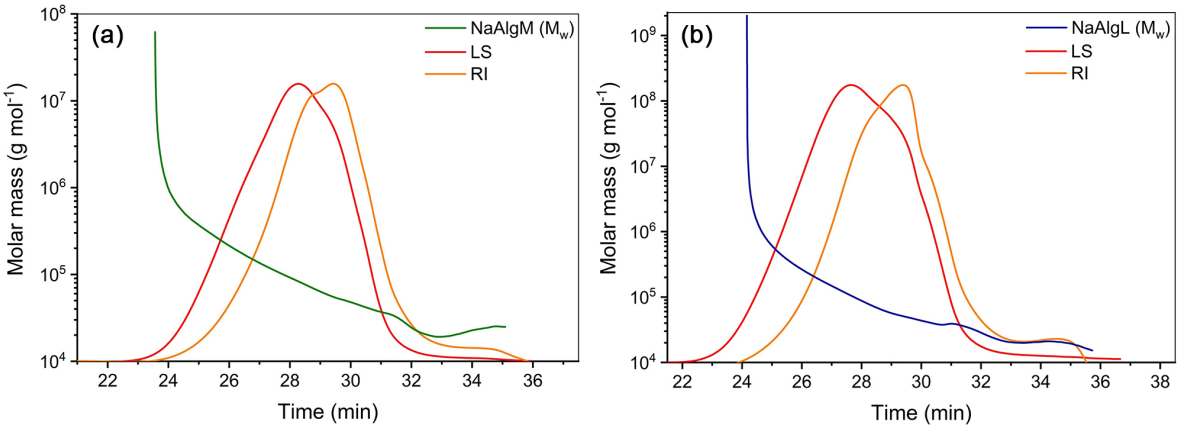

Figure 4. SEC-MALS chromatograms of sodium alginate samples extracted from (a) *M. pyrifera* (NaAlgM) and (b) *L. trabeculata* (NaAlgL). Refractive index (RI, orange line); light scattering at angle of 90° (LS, red line); and molecular weight distribution for NaAlgM (green line) and NaAlgL (blue line).

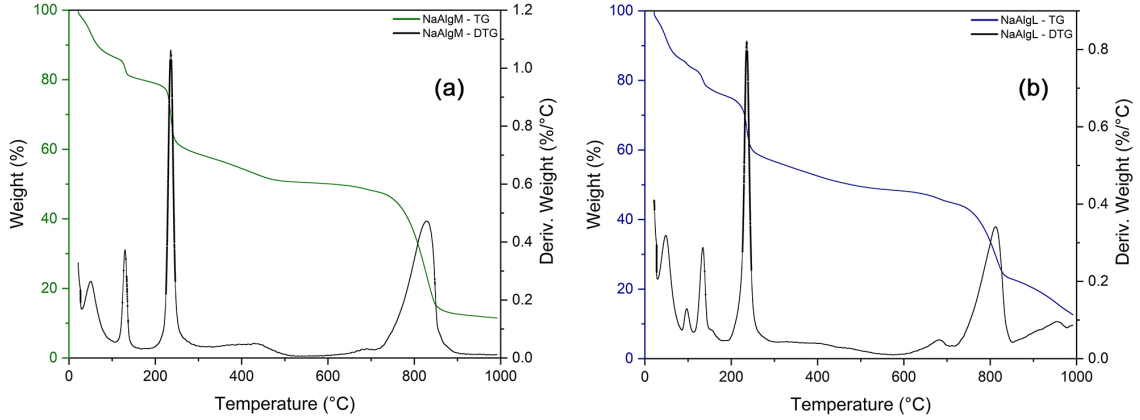

Figure 5. TG/DTG curves of sodium alginate samples extracted from (a) *M. pyrifera* (NaAlgM) and (b) *L. trabeculata* (NaAlgL).

Fourier-transform infrared spectroscopy

The FTIR spectrum of NaAlgM and NaAlgL (Figure 6) show a broad peak at 3270 cm^{-1} attributed to the stretching vibrations of hydroxyl groups O–H[36] and others at 2929, 1728, 1595 and 1024 cm^{-1} were attributed to aliphatic –CH stretching,[37] the carbonyl group as the carboxylic acid ester form (C=O),[22] carboxylate O–C–O asymmetric stretching vibrations,[38] and stretching vibration of C–O–C,[39] respectively.

The absorption at 1352 cm^{-1} corresponding to the vibration of S=O stretching,[40] and the presence of fucoidan sulfate groups at 835 cm^{-1} was reported.[41] Also, the band around 665 cm^{-1} is attributed to C–H bending vibration, confirming the presence of carbohydrates.[42]

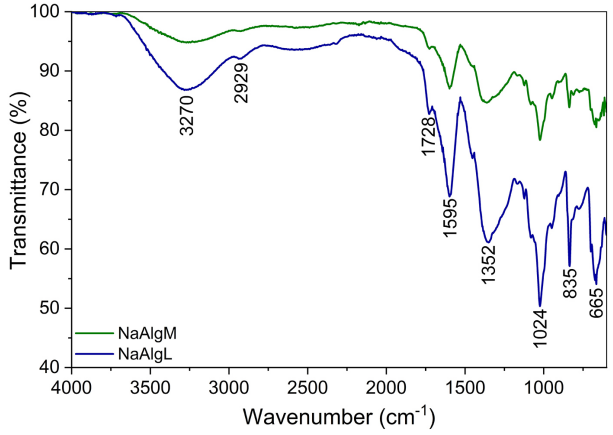

Figure 6. FTIR (ATR) spectrum of sodium alginate samples extracted from *M. pyrifera* (NaAlgM, green line) and *L. trabeculata* (NaAlgL, blue line).

X-ray diffraction

XRD diffractograms of the sodium alginate samples (Figure 7) have two diffraction peaks at 14.08 and 22.08°[43] corresponding to the units of guluronate (G) and mannuronate (M), respectively.[44] The crystallinity index (Table 5) of the NaAlgM and NaAlgL samples is 20.19 and 17.31%, respectively. According to Helmiyati and Aprilliza,[45] the crystallinity index in sodium alginate samples extracted is close to 29.29%, showing low purity in the alginate samples obtained. In one hand, a sharp peak at 29.5°, and other peaks at 34, 39, 44, and 48° were observed in the diffractogram of the samples. For another hand, these last signals correspond to $CaCO_3$;[46] therefore, it was presumed that this salt was formed during the extraction process.

Composite films sodium alginate-based elaborated

Two composite films of sodium alginate-based were prepared: the first with sodium alginate from *Macrocystis pyrifera* was called F_1, and the other with sodium alginate from *Lessonia trabeculata* was called F_2.

Fourier-transform infrared spectroscopy of films

The FTIR spectrum of the films (Figure 8a) shows a peak at 2879 cm^{-1} corresponding to C–H stretching,[47] and others at 1605 and 1409, 1350, and 1244 cm^{-1} were attributed to asymmetric and symmetric stretching of the carboxylate group,[43] aliphatic C–H stretching of plasticizers,[48] and C–OH stretching,[49] respectively. The peak at 1029 cm^{-1} is associated with the S=O vibrational mode due to the presence of carrageenans[50] and the O–H bond vibration; 923 cm^{-1} corresponds to the C–H bond[51] and the presence of 3,6-anhydro-D-galactose; and at 848 cm^{-1} is assigned to D-galactose-4-sulfate.[52]

X-ray diffraction of films

The XRD diffractogram (Figure 8b) shows the diffraction pattern of the films at 21° and the disappearance

Table 4. Mass loss values from TG/DTG curves of sodium alginate samples extracted from *M. pyrifera* (NaAlgM) and *L. trabeculata* (NaAlgL)

Sample	Mass / mg	Thermal event	ΔT / °C	Mass loss / %	Residue / %
NaAlgM	5.308	dehydration	21.7-182.3	20.4	
		fragmentation	182.3-542.0	29.1	
		decomposition	542.0-907.1	38.0	
		carbonization	907.1-991.3	1.3	
		carbonized residue	991.3		11.2
NaAlgL	5.114	dehydration	21.5-180.9	23.5	
		fragmentation	180.9-574.3	27.4	
		decomposition	574.3-853.3	26.0	
		carbonization	853.3-991.8	10.2	
		carbonized residue	991.8		12.9

T: temperature.

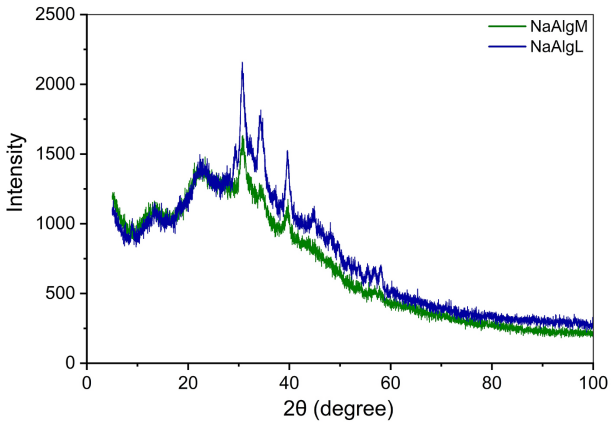

Figure 7. XRD diffractograms of sodium alginate samples extracted from *M. pyrifera* (NaAlgM, green line) and *L. trabeculata* (NaAlgL, blue line).

of the peak close to 13°, which is according to the literature[53,54] and shows that there is no destruction in the crystal structure of sodium alginate.[55] On the other hand, the films presented a crystallinity index of 36.17% for F_1 film and 28.40% for F_2 film; which could mean the formation of crystalline microaggregates due to the electrostatic interaction between the amino groups of the AVG and the carboxyl groups of sodium alginate.[56]

Table 5. XRD data of guluronate (G) and mannuronate (M) units, and crystallinity of sodium alginate samples extracted from *M. pyrifera* (NaAlgM) and *L. trabeculata* (NaAlgL)

Sample	2θ / degree		Crystallinity / %
	G	M	
NaAlgM	13.35	23.35	20.19
NaAlgL	13.29	22.31	17.31

Thermogravimetry of films

Figure 9 shows the TG/DTG thermogravimetric curves of the films. Both films show similar thermal decomposition patterns with four thermal events ranging from 25 to 1000 °C (Table 6). According to Bhatia *et al.*,[57] the first event is attributed to the evaporation of water bound to the film, and the second event is to the loss of plasticizers. However, Wai Chun *et al.*[58] consider that the second event refers to the fragmentation of the films, which shows a more significant mass loss. The third event is

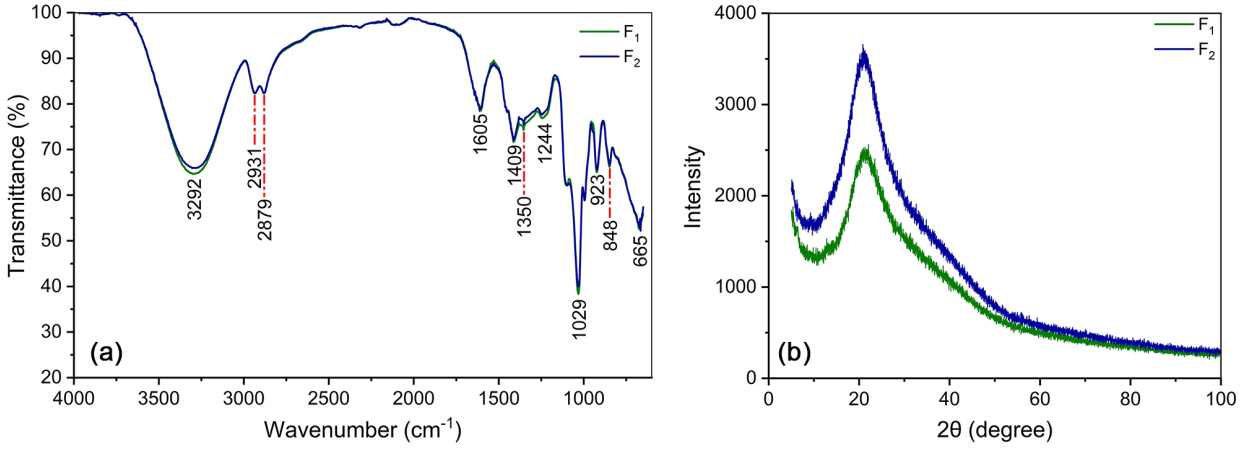

Figure 8. (a) FTIR (ATR) spectra, and (b) XRD diffractograms of F_1 and F_2 films.

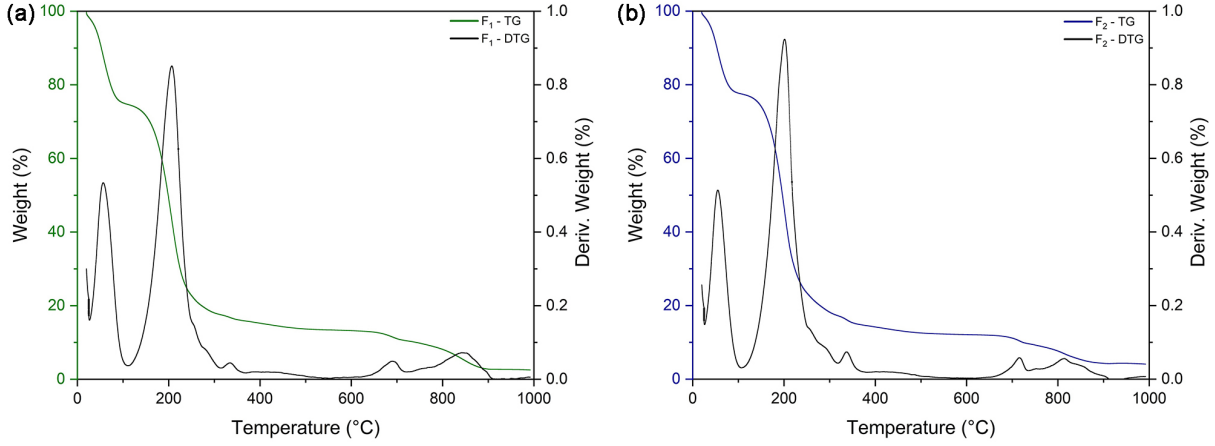

Figure 9. TG/DTG curves of (a) F_1 and (b) F_2 films.

Table 6. Mass loss values from TG/DTG curves of F_1 and F_2 films

Sample	Mass / mg	Thermal event	ΔT / °C	Mass loss / %	Residue / %
F_1	6.053	dehydration	20.0-110.0	25.3	
		fragmentation	110.0-313.8	57.2	
		decomposition	313.8-551.3	4.1	
		carbonization	551.3-991.8	11.0	
		carbonized residue	991.8		2.4
F_2	6.299	dehydration	19.7-105.6	22.1	
		fragmentation	105.6-316.7	60.3	
		decomposition	316.7-617.3	5.2	
		carbonization	617.3-990.1	8.0	
		carbonized residue	990.1		4.4

T: temperature.

associated with the decomposition of the organic structure of the polysaccharides, and the last event indicates the carbonization process of the carbonaceous material.[59]

Surface morphology analysis

The surface morphology analysis (SEM) images of the films loaded with an AVG ethanolic solution (Figure 10) revealed a homogeneous surface with slight roughness, especially in the F1 film, due to ethanol generating a positive impact on the homogeneity and visual appearance of the films.[60] The F_2 film has a smoother and more homogeneous surface, which indicates an adequate interaction between the polymeric matrices, the plasticizers, and the drug (AVG).[61]

Kinetic behavior of AVG release

Figure 11 shows the release profile of AVG over 7 h at 10 and 25 °C. At 10 °C, F_1 film released 18.60 mg L^{-1} (93.02%) and F_2 film 14.21 mg L^{-1} (71.06%) of AVG; and at 25 °C, F_1 film released 10.97 mg L^{-1} (54.85%) and F_2 film 13.81 mg L^{-1} (69.04%) of AVG. This shows that films release a higher AVG content at low temperatures because there is a lower crosslink density which increased pores in the film's polymer network.[62] However, when ethanol was used as a release medium, swelling of the film was inhibited.[60]

Table 7 shows the values of the correlation coefficient (R^2) and the diffusion exponent (n) calculated from equations 2 and 3. At 10 °C, the Korsmeyer-Peppas model better describes AVG release because it has a higher R^2 value than the Higuchi model. However, the Higuchi model better describes the release at 25 °C because it has a higher R^2 value at this temperature. On the other hand, the value of n is less than 0.5, so it is assumed that the release of AVG at both temperatures corresponds to a diffusion controlled by Fick's law.

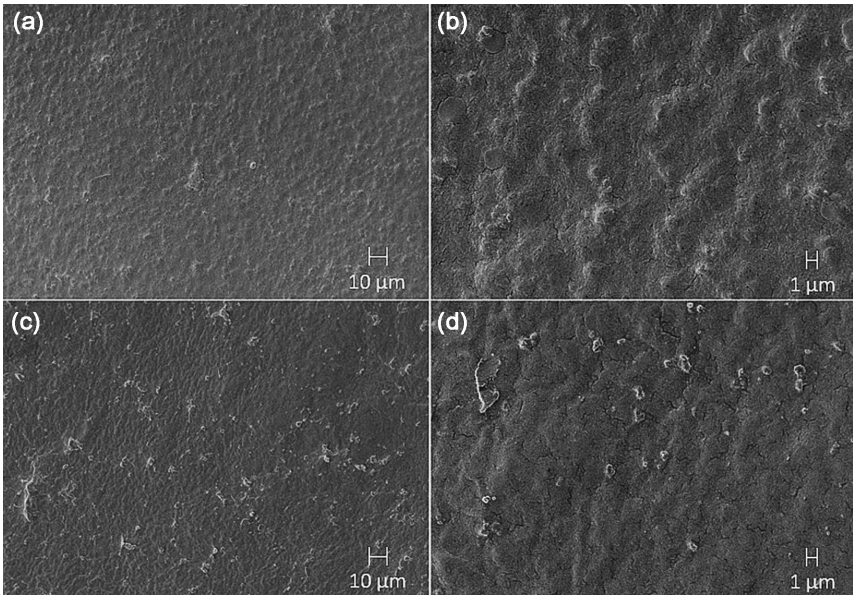

Figure 10. SEM images at (a) 1.00 k× (10 µm) and (b) 5.00 k× (1 µm) magnification on F_1 film and (c) 1.00 k× (10 µm) and (d) 5.00 k× (1 µm) on F_2 film.

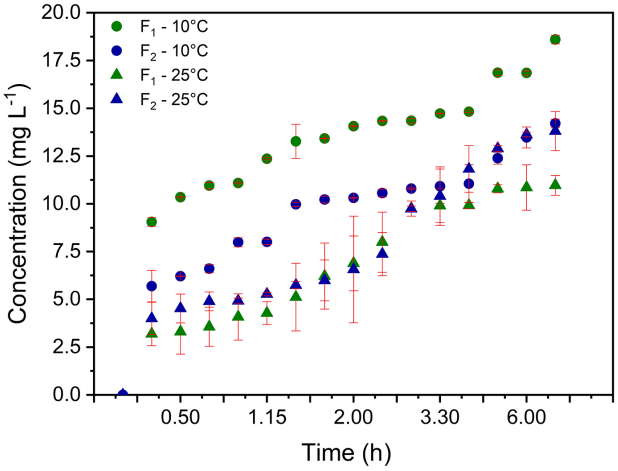

Figure 11. Release profiles at 10 and 25 °C of AVG loaded on F_1 and F_2 films.

Table 7. Kinetic parameters obtained by the method of Higuchi and Korsmeyer-Peppas

Film	Temperature / °C	Higuchi	Korsmeyer-Peppas	
		R^2	n	R^2
F_1	10	0.8034	0.1721	0.9504
F_1	25	0.9419	0.4016	0.9038
F_2	10	0.8858	0.2415	0.9538
F_2	25	0.9512	0.3627	0.8613

R^2: correlation coefficient; n: diffusion exponent.

Conclusions

In the present study, sodium alginates extracted from *Macrocystis pyrifera* and *Lessonia trabeculata* species had low extraction yield, low crystallinity index, low average molar mass, and the possible presence of $CaCO_3$, carbohydrates, and fucoidans. The films prepared with these sodium alginate samples presented a homogeneous surface with slight roughness, which suggests an interaction between sodium alginate, carrageenan, plasticizers, and aminoethoxyvinylglycine; however, at low temperatures and governed by Fick's law, they released a greater amount of AVG. Therefore, these films can be an alternative for fruit packaging at 10 °C since they serve as vehicles for the administration and release of ethylene inhibitor. In general, polysaccharides from algae allow the production of films that can replace synthetic plastics.

Acknowledgments

The authors thank the Peruvian government for funding the research through the Prociencia/World Bank program project grant 01-2018-FONDECYTBM-IADTUM.

Author Contributions

The authors contributed equally to the written and experimental part of the manuscript.

References

1. Kanagesan, K.; Abdulla, R.; Derman, E.; Sabullah, M.; Govindan, N.; Gansau, J.; *J. King Saud Univ., Sci.* **2022**, *34*, 102268. [Crossref]
2. Jayakody, M. M.; Vanniarachchy, M. P. G.; Wijesekara, I.; *J. Food Meas. Charact.* **2022**, *16*, 1195. [Crossref]
3. Faidi, A.; Stumbé, J. F.; Safta, F.; Sfar, S.; *J. Food Meas. Charact.* **2022**, *16*, 4457. [Crossref]
4. Barbut, S.; Harper, A.; *LWT* **2019**, *103*, 260. [Crossref]
5. Permatasari, A. A. A. P.; Rosiana, I.; Wiradana, P.; Lestari, M.; Widiastuti, N.; Kurniawan, S. B.; Widhiantara, I.; *Biodiversitas* **2022**, *23*, 1656. [Crossref]
6. Fertah, M.; Belfkira, A.; Dahmane, E.; Taourirte, M.; Brouillette, F.; *Arabian J. Chem.* **2017**, *10*, S3707. [Crossref]
7. Baek, S.-K.; Kim, S.; Song, K. B.; *Int. J. Mol. Sci.* **2018**, *19*, 3545. [Crossref]
8. Pacheco-Quito, E. M.; Ruiz-Caro, R.; Veiga, M.-D.; *Mar. Drugs* **2020**, *18*, 583. [Crossref]
9. Jancikova, S.; Dordevic, D.; Jamroz, E.; Behalova, H.; Tremlova, B.; *Foods* **2020**, *9*, 357. [Crossref]
10. Prasetyaningrum, A.; Utomo, D. P.; Raemas, A. F. A.; Kusworo, T. D.; Jos, B.; Djaeni, M.; *Polymers* **2021**, *13*, 354. [Crossref]
11. Sedayu, B. B.; Cran, M. J.; Bigger, S. W.; *Carbohydr. Polym.* **2019**, *216*, 287. [Crossref]
12. Siracusa, V.; Romani, S.; Gigli, M.; Mannozzi, C.; Cecchini, J. P.; Tylewicz, U.; Lotti, N.; *Materials* **2018**, *11*, 1980. [Crossref]
13. Gaikwad, K. K.; Singh, S.; Negi, Y. S.; *Environ. Chem. Lett.* **2020**, *18*, 269. [Crossref]
14. Elmenofy, H. M.; Okba, S. K.; Salama, A.-M.; Alam-Eldein, S. M.; *Plants* **2021**, *10*, 1838. [Crossref]
15. Schaller, G. E.; Binder, B. M. In *Methods in Molecular Biology*, vol. 1573; Walker, J. M., ed.; Springer: USA, 2017, p. 223. [Crossref]
16. Gómez, C. G.; Pérez, M. V. P.; Lozano, J. E.; Rinaudo, M.; Villar, M. A.; *Int. J. Biol. Macromol.* **2009**, *44*, 365. [Crossref]
17. Cha, D. S.; Choi, J. H.; Chinnan, M. S.; Park, H. J.; *LWT* **2002**, *35*, 715. [Crossref]
18. Paula, G. A.; Benevides, N. M. B.; Cunha, A. P.; de Oliveira, A. V.; Pinto, A. M. B.; Morais, J. P. S.; Azeredo, H. M. C.; *Food Hydrocoll.* **2015**, *47*, 140. [Crossref]
19. Khan, M. U. A.; Yaqoob, Z.; Ansari, M. N. M.; Razak, S. I. A.; Raza, M. A.; Sajjad, A.; Haider, S.; Busra, F. M.; *Polymers* **2021**, *13*, 3124. [Crossref]
20. Postolović, K. S.; Antonijević, M. D.; Ljujić, B.; Radenković, S.; Kovačević, M. M.; Hiezl, Z.; Pavlović, S.; Radojević, I.; Stanić, Z.; *Polymers* **2022**, *14*, 4091. [Crossref]

21. Rashedy, S. H.; Abd El Hafez, M. S. M.; Dar, M. A.; Cotas, J.; Pereira, L.; *Appl. Sci.* **2021**, *11*, 6290. [Crossref]
22. Belattmania, Z.; Kaidi, S.; El Atouani, S.; Katif, C.; Bentiss, F.; Jama, C.; Reani, A.; Sabour, B.; Vasconcelos, V.; *Molecules* **2020**, *25*, 4335. [Crossref]
23. ASTM F2605-16: *Standard Test Method for Determining the Molar Mass of Sodium Alginate by Size Exclusion Chromatography with Multi-angle Light Scattering Detection (SEC-MALS)*, West Conshohocken, 2016.
24. Kaidi, S.; Bentiss, F.; Jama, C.; Khaya, K.; Belattmania, Z.; Reani, A.; Sabour, B.; *Colloids Interfaces* **2022**, *6*, 51. [Crossref]
25. Rioux, L.-E.; Turgeon, S. L.; Beaulieu, M.; *Carbohydr. Polym.* **2007**, *69*, 530. [Crossref]
26. Dobrinčić, A.; Balbino, S.; Zorić, Z.; Pedisić, S.; Kovačević, D. B.; Garofulić, I. E.; Dragović-Uzelac, V.; *Mar. Drugs* **2020**, *18*, 168. [Crossref]
27. Murillo-Álvarez, J. I.; Hernández-Carmona, G.; *J. Appl. Phycol.* **2007**, *19*, 545. [Crossref]
28. Venegas, M.; Matsuhiro, B.; Edding, M. E.; *Bot. Mar.* **1993**, *36*, 47. [Crossref]
29. McKee, J. W. A.; Kavalieris, L.; Brasch, D. J.; Brown, M.; Melton, L. D.; *J. Appl. Phycol.* **1992**, *4*, 357. [Crossref]
30. Sperger, D. M.; Fu, S.; Block, L. H.; Munson, E. J.; *J. Pharm. Sci.* **2011**, *100*, 3441. [Crossref]
31. Urbanova, M.; Pavelkova, M.; Czernek, J.; Kubova, K.; Vyslouzil, J.; Pechova, A.; Molinkova, D.; Vyslouzil, J.; Vetchy, D.; Brus, J.; *Biomacromolecules* **2019**, *20*, 4158. [Crossref]
32. Deng, Y.; Yang, N.; Okoro, O.; Shavandi, A.; Nie, L. In *Properties and Applications of Alginates*; Deniz, I.; Imamoglu, E.; Keskin-Gundogdu, T., eds.; IntechOpen, 2021, ch. 6. [Crossref]
33. Popovici, S.-T.; Kok, W. T.; Schoenmakers, P. J.; *J. Chromatogr. A* **2004**, *1060*, 237. [Crossref]
34. Boucelkha, A.; Petit, E.; Elboutachfaiti, R.; Molinié, R.; Amari, S.; Zaidi-Yahaoui, R.; *J. Appl. Phycol.* **2017**, *29*, 509. [Crossref]
35. Kragović, M.; Daković, A.; Marković, M.; Petković, A.; *Zaštita materijala* **2016**, *57*, 559. [Crossref]
36. Al Monla, R.; Dassouki, Z.; Sari-Chmayssem, N.; Mawlawi, H.; Gali-Muhtasib, H.; *Molecules* **2022**, *27*, 358. [Crossref]
37. Mahcene, Z.; Khelil, A.; Hasni, S.; Akman, P.; Bozkurt, F.; Birech, K.; Goudjil, M.; Tornuk, F.; *Int. J. Biol. Macromol.* **2020**, *145*, 124. [Crossref]
38. Fenoradosoa, T. A.; Ali, G.; Delattre, C.; Laroche, C.; Petit, E.; Wadouachi, A.; Michaud, P.; *J. Appl. Phycol.* **2010**, *22*, 131. [Crossref]
39. Liu, S.; Li, Y.; Li, L.; *Carbohydr. Polym.* **2017**, *160*, 62. [Crossref]
40. Badrinathan, S.; Shiju, T.; Sharon Christa, A.; Arya, R.; Pragasam, V.; *Indian J. Pharm. Sci.* **2012**, *74*, 549. [PubMed]
41. Qiu, X.; Amarasekara, A.; Doctor, V.; *Carbohydr. Polym.* **2006**, *63*, 224. [Crossref]
42. Anand, M.; Suresh, S.; *Adv. Nat. Sci.: Nanosci. Nanotechnol.* **2015**, *6*. [Crossref]
43. Zheng, H.; Yang, J.; Han, S.; *J. Appl. Polym. Sci.* **2016**, *133*, 43616. [Crossref]
44. Sundarrajan, P.; Eswaran, P.; Marimuthu, A.; Subhadra, L.; Kannaiyan, P.; *Bull. Korean Chem. Soc.* **2012**, *33*, 3218. [Crossref]
45. Helmiyati; Aprilliza, M.; *IOP Conf. Ser.: Mater. Sci. Eng.* **2017**, *188*, 012019. [Crossref]
46. Jiang, Y.; Pang, X.; Deng, Y.; Sun, X.; Zhao, X.; Xu, P.; Shao, P.; Zhang, L.; Li, Q.; Li, Z.; *Polymers* **2019**, *11*, 1973. [Crossref]
47. Kongjao, S.; Damronglerd, S.; Hunsom, M.; *Korean J. Chem. Eng.* **2010**, *27*, 944. [Crossref]
48. Shameli, K.; Ahmad, M.; Jazayeri, S.; Sedaghat, S.; Shabanzadeh, P.; Jahangirian, H.; Mahdavi, M.; Abdollahi, Y.; *Int. J. Mol. Sci.* **2012**, *13*, 6639. [Crossref]
49. Khairuddin; Pramono, E.; Utomo, S.; Wulandari, V.; Zahrotul, A.; Clegg, F.; *J. Phys.: Conf. Ser.* **2016**, *776*, 012053. [Crossref]
50. Karthikeyan, S.; Selvasekarapandian, S.; Premalatha, M.; Monisha, S.; Boopathi, G.; Aristatil, G.; Arun, A.; Madeswaran, S.; *Ionics* **2016**, *23*, 2775. [Crossref]
51. Abbasiliasi, S.; Shun, T.; Tengku Ibrahim, T.; Ismail, N.; Ariff, A.; Mokhtar, N.; Mustafa, S.; *RSC Adv.* **2019**, *9*, 16147. [Crossref]
52. Pereira, L.; Gheda, S.; Ribeiro-Claro, P. J. A.; *Int. J. Carbohydr. Chem.* **2013**, ID 537202. [Crossref]
53. Al-Harrasi, A.; Bhatia, S.; Al-Azri, M.; Ullah, S.; Najmi, A.; Albratty, M.; Meraya, A.; Mohan, S.; Aldawsari, M. F.; *Membranes* **2022**, *12*, 862. [Crossref]
54. Ci, M.; Liu, J.; Liu, L.; Shang, S.; Zhang, G.; Zhu, P.; Sui, S.; *J. Phys.: Conf. Ser.* **2021**, *1790*, 012073. [Crossref]
55. Mutlu, B.; Farhan, M.; Kucuk, I.; *Polymers* **2019**, *11*, 1386. [Crossref]
56. Rezvanian, M.; Amin, M. C. I. M.; Ng, S.-F.; *Carbohydr. Polym.* **2016**, *137*, 295. [Crossref]
57. Bhatia, S.; Al-Harrasi, A.; Al-Azri, M.; Ullah, S.; Bekhit, A. E. A.; Pratap-Singh, A.; Chatli, M.; Anwer, M.; Aldawsari, M. F.; *Polymers* **2022**, *14*, 3855. [Crossref]
58. Wai Chun, C. N.; Tajarudin, H. A.; Ismail, N.; Azahari, B.; Makhtar, M. M. Z.; *Polymers* **2021**, *13*, 2103. [Crossref]
59. Azucena Castro-Yobal, M.; Contreras-Oliva, A.; Saucedo-Rivalcoba, V.; Rivera-Armenta, J.; Hernández-Ramírez, G.; Salinas-Ruiz, J.; Herrera-Corredor, A.; *e-Polymers* **2021**, *21*, 82. [Crossref]
60. Li, J.; He, J.; Huang, Y.; Li, D.; Chen, X.; *Carbohydr. Polym.* **2015**, *123*, 208. [Crossref]
61. de Farias, Y. B.; Coutinho, A. K.; Assis, R. Q.; Rios, A O.; *J. Food Process Eng.* **2020**, *43*, e13345. [Crossref]
62. Kopač, T.; Krajnc, M.; Ručigaj A.; *Int. J. Biol. Macromol.* **2021**, *168*, 695. [Crossref]

Submitted: December 14, 2022
Published online: May 2, 2023